inter·noise 96
25th Anniversary Congress – Liverpool

INCE: 42

STRUCTURE-BORNE SOUND PREDICTION AND CONDUCTIVITY MODELLING FOR AN INFINITE REINFORCED PLATE STRUCTURE

M Smith

Martec Limited, 400-1888 Brunswick Street, Halifax NS, Canada

1. INTRODUCTION

The structural-acoustic behaviour of an infinite beam-plate system is considered (Fig. 1). Wave propagation and power input characteristics are first discussed for varying beam size. Conductivity modelling of the plate and beam is then investigated as part of a continuing effort to develop relatively simple models for energy flow in complex structures. A model for the attached plate is developed based on the farfield energy distribution in an unstiffened plate with a point load.

2. PHYSICAL BEHAVIOUR

Dispersion Relation

Lamb [1] derived a dispersion relation for flexural motion of a beam with an attached plate, the roots of which define the wave constants of the beam motion. Generally, these occur as complex pairs corresponding to oppositely directed waves which are either predominantly propagating or predominantly evanescent [2].

Fig. 2 shows the wave constant for the predominantly propagating wave mode for various beam sizes determined by Newton-Raphson iteration. The beam has width b, depth d and a b/d ratio of 0.2; the plate thickness t is 2cm and the frequency is 120 Hz. With very light beams the wave modes are the same as those of the plates; but at $d/t = 2.5$ an abrupt transition to beam-like behaviour occurs. At intermediate beam sizes the evanescent component is about 10-20% of the propagating component, resulting in sharp attenuation of the flexural waves. Physically, this is caused by wave energy radiating to the adjoining plate. The group velocity of the propagating mode (Fig. 3) shows a linear dependence on the beam depth, in contrast to the familiar square root dependency of the free-beam wave mode.

Input Power

The input power due to a point harmonic force is proportional to the real part of the driving point mobility β of the system. The mobility can be obtained either by numerically inverting its Fourier transform and evaluating it at the driving point or by using the first order approximation given by Skudryzk [3]:

$$\beta = (Z_b+Z_p)^{-1} \qquad (1)$$

where Z_b and Z_p are the driving point impedances of the uncoupled beam and plate, respectively. In Fig. 4 the input power is plotted as a fraction of the power into an unstiffened plate of the same size, under the same loading. At intermediate beam sizes, the mobility approximation causes the input power to be overestimated by as much as 50%.

3. CONDUCTIVITY MODELLING

Beam Modelling

The radiation of energy from beam to the plate has been previously given by [4]:

$$q_r = \gamma c_b \langle e_b \rangle \qquad (2)$$

where q_r is the power radiated per unit length, γ is a radiation parameter, c_b is the group velocity (Fig. 3), and $\langle e_b \rangle$ is the time-averaged flexural energy density on the beam. The conductivity model predicts a farfield energy density of

$$\langle e_b \rangle = (P_{in}/2c_b)\exp\{-\alpha_b|x|\} \qquad \alpha_b = \omega\eta/c_b+\gamma = -2\mathrm{Im}\{k_1\} \qquad (3)$$

where $\mathrm{Im}\{k_1\}$ is the evanescent part of wave constant in the propagation mode. The last equality in (3) defines the radiation parameter such that the decay rate in the model matches that observed for free waves in Fig. 2. Satisfactory results were obtained in the farfield with this approach [4]. No information about the nearfield response, however, is retained in the conductivity model, so the technique is not useful for predicting the velocity near the driving point.

Plate Modelling

The plate velocity amplitude shown in Fig. 5 was obtained by numerical inversion of the Fourier transform expressions obtained by Goyder and White [5], for the case $d/t = 20$. The x and y axes in this figure are in units of wavelengths. A significant feature is the decay along the beam axis ($y=0$), at a rate of $8.69\mathrm{Im}\{k_1\}$ dB/m. Another is the pair of ridges radiating from the driving point at angles equal to the trace-matching angle for flexural waves on the beam and plate, a feature noted by

Kovinskaya and Nikiforov [6]. Numerical analysis has shown that between these two ridges the plate velocity is a cylindrical wave pattern centred on the driving point; to either side of the ridges is a plane wave field propagating at the trace-matching angle.

Conductivity models previously used were suitable for diffuse fields on finite plates [4]. The approach used here for infinite plates is based on the known farfield energy density in the absence of a stiffener:

$$\frac{\langle e_p(r) \rangle}{P_{in}} = \frac{\exp\{-(\omega\eta/c_p)r\}}{2\pi r c_p} \qquad (4)$$

where P_{in} is the power input due to a point force and r is the radial distance from the driving point. For a plate excited through a stiffener, power enters the plate not at a point, but as a continuous distribution along the beam axis. Using the right-hand side of (4) as the Green's function of the plate response and (2) as the power input function, the plate energy density becomes

$$\langle e_p(x,y) \rangle = \int_{-\infty}^{\infty} \frac{\gamma c_b \langle e_b(\xi) \rangle \exp\left\{-(\omega\eta/c_p)\sqrt{(x-\xi)^2+y^2}\right\}}{2\pi c_p \sqrt{(x-\xi)^2+y^2}} \, d\xi \qquad (5)$$

Substituting the expression for $\langle e_b \rangle$ in (3), the integral can be evaluated numerically. Results are shown in Fig. 6 in which the velocity level is normalized to the peak value in Fig. 5. The plate response near the driving point and along the axis $x = 0$ (perpendicular to the beam axis) is predicted quite accurately. The response along the beam axis ($y = 0$) is about 3 dB too high, but the rate of decay away from the driving point is almost the same as in Fig. 5. The model, however, is not capable of predicting the pair of ridges caused by the interference between plane and cylindrical wave fields. In using (5) it is assumed that the total energy is just the sum of the energy fields produced at each source point. For plate energies to be additive, the energy densities must be time-averaged and locally space-averaged quantities, hence precluding the modelling of phase or interference effects.

An integral expression for the plate intensity can be obtained in a similar way. Further development of the method should enable it to be applied to more complex plate-beam systems.

References

[1] G.L.Lamb, J. Acoust. Soc. Am., 33, 628 (1961).
[2] F.J.Fahy and E.Lindqvist, J. Sound Vib., 45, 115 (1976).
[3] E.Skudrzyk, J. Acoust. Soc. Am., 67(4), 1105 (1980).
[4] M.J.Smith and M.J.Chernuka, Proc. 14th Mech. Vib. Sem., CMVA, 80 (1995).
[5] H.G.D.Goyder and R.G.White, J. Sound Vib, 68, 77 (1980).
[6] S.I.Kovinskaya and A.S.Nikiforov, Sov. Phys. Acous., 19, 32 (1973).

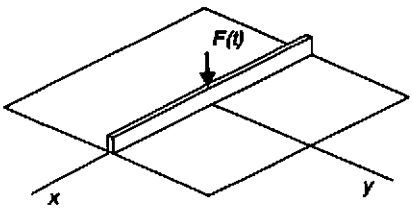

Figure 1. Point-loaded beam-plate system.

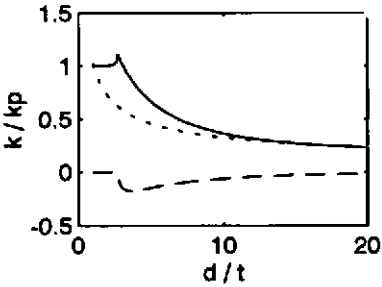

Figure 2. Coupled beam wave constant: (—) real part; (— —) imag part; (- -) free beam.

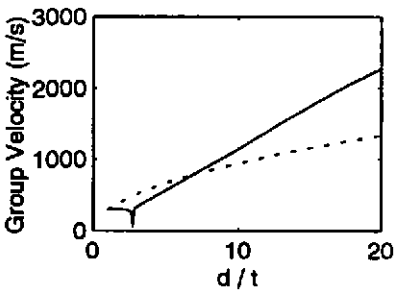

Figure 3. Group velocity. (—) coupled beam; (- -) free beam.

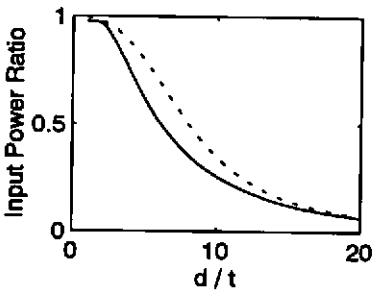

Figure 4. Input power: (—) numerical integration; (- -) mobility approximation.

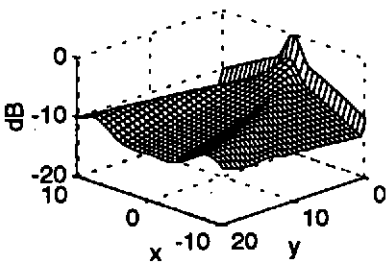

Figure 5. Plate velocity amplitude, d/t = 20.

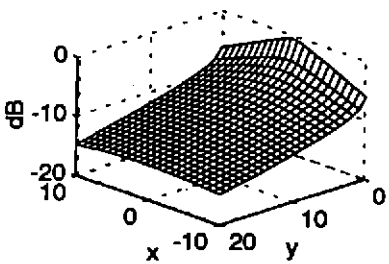

Figure 6. Plate velocity amplitude from conductivity model, d/t = 20.